Wire Bonding Failure Characterization of an IGBT Based Power Module Through Impedance Analysis

Paul-Etienne Vidal, Stéphane Baffreau, Guillaume Viné,
Anusha Gopishetti and Than-Long Le

September 13, 2024

Wire bonding failure characterization of an IGBT based power module through impedance analysis

P.-E. Vidal[a,b,c,*], S. Baffreau[b,c], G. Viné[b,c], A. Gopishetti[d], T.L. Long[e]

[a] *Université de Pau et Pays de l'Adour(UPPA), Pau, France*
[b] *Laboratoire Génie de Production, Université de Technologie de Tarbes, France*
[c] *Toulouse University, France*
[d] *DEEPConcept, Pau, France*
[e] *SafranTech, Paris Saclay, France*
[*] *corresponding author*

Abstract

This study deals with the development of a wide-frequency-band characterization for failure analysis of power modules, focusing on a specific IGBT packaging. It is highlighted that different characteristics of the IGBT and the packaging can be distinguished depending on the frequency band analyzed, enabling the detection of potential failure modes. Particularly, for the power bond-wire lift-off mechanism, the paper emphasizes the importance of considering high-frequency analysis above 200 MHz. It is enabled through the definition of a failure indicator, demonstrating the ability to highlight partial failures as well as to localize them.

1. Introduction

The electrical energy conversion is crucial for addressing the social goal of green transition. This transformation is made possible through the use of static converters relying on semiconductor switches. In particular, the development of medium and high-power electrical applications, such as renewable energy networks and electric transportation, underscores the necessity for a greater array of power converters with enhanced performances, in terms of voltage/current ratings, and capable of operating in harsh environments (thermic, electromagnetic disturbances, etc.). Within these medium and high-power applications, the fundamental building block of the converter is the power module which integrates multiple power semiconductors' switches into a unified package. Given its critical role in the power converter, one of the prevailing scientific challenges lies in enhancing the reliability of the power modules to extend their lifetime and in developing effective failure detection methodologies for a proactive maintenance strategy.

In power modules, the failures can be originated from an active element (semiconductor), or a passive element (ceramic substrate, interconnections, brazing etc.) of the assembly, [1]. The package health monitoring can be obtained with a degradation indicator usually linked to the measurement of an electrical variable (current or voltage), [2]. However, devising a comprehensive method that is non-destructive and capable of detecting all failure modes remains a challenging endeavor. This paper addresses this challenge through the development of a Non-Destructive Testing (NDT) method which relies on wide frequency band impedance measurement of the power module [3]. It is predicated on the assumption that impedance variations arise from various failure mechanisms within the power module [4].

Firstly, the paper describes the device under test, an IGBT-based power module. Secondly, the protocol established to characterize the device is presented. Subsequently, the NDT methodology is applied to a healthy and faulty states module, emphasizing the distinct influences of both the IGBT and the packaging. The NDT is tested on degraded packaging where power bond-wires are manually lifted-off. The experimental results obtained allow us to identify the change in the impedance behavior following the number of wire bonding failures. Moreover, the paper proposes and analyses a specific failure indicator.

2. Power module setup and characterization

2.1. Power module description

A homemade power module assembly is achieved as illustrated in Fig. 1. It is composed of an IGBT referenced FGH25T120SM, from Fairchild semiconductors, rated at 1200 V and 25 A. The collector metallization pad is brazed (SnAgCu) onto the top side of a metallized ceramic substrate. The connections from the top of the IGBT, emitter and gate ports, to the substrate is ensured by, respectively, 5 and 1 aluminum bonding wires of 300 μm diameter. Consequently, the tracks TG, TC and TE of the substrate are connected to the gate, collector and emitter ports of the IGBT respectively. The ceramic substrate, 0.32 mm thick, is made of Si_3N_4 with thick copper tracks of 0.225 mm, on top and bottom sides.

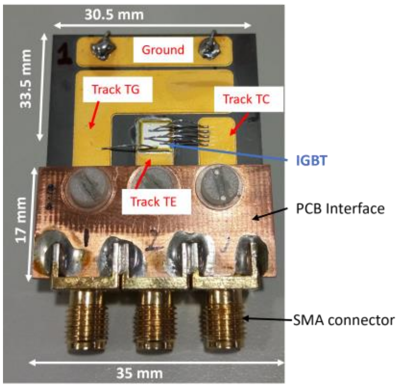

Fig. 1 IGBT based power module assembly – top view

2.2. Impedance measurement interface

As presented in Fig. 1, to perform the high frequency characterization, a PCB interface, made of an FR4-epoxy, 1.6 mm thick, and copper tracks, 35 µm thick, is designed. Its connection to a Vector Network Analyzer (VNA) is achieved thanks to 3 Sub-Miniature of Type A connectors (SMA). The three measurement ports are thus connected to the tracks TG, TC and TE of the device.

2.3. RF characterization process

The impedance parameters (Z-parameters) are obtained through an off-line post-processing process based on VNA measurements. The VNA (Keysight E5061B) allows the characterization of scattering–parameters (S-parameters) in two-port networks. The S-parameters measurement and the off-line conversion process, detailed below, relies on the use of S-parameters, which are widely used to describe the RF behavior of linear electrical networks like electronic circuits or components (with "small signals" hypothesis). The S-parameters establish relationships between their input/output ports in terms of wave power reflection and transmission [5].

Before any measurement, a two-ports calibration has been performed. For every port, the calibration process is done in three steps: open, short and match loads Then, a thru measurement is done between ports. The RF methodology involves experimentations and data-based computations as detailed in [3]. The main steps are:

Step 1: Calibration phase, followed by the S-parameters measurement onto the device.

Step 2: S–parameters to Z–parameters off-line conversion based on network theory [6].

Step 3: S- and Z-parameters analyses.

2.4. Power wire-bonds failure application

The healthy mode represents the initial status of the power module without any induced degradation. This study focuses on the degradation mechanism of power wire-bonds lift-off, a significant mode of degradation primarily occurring at the top connections of semiconductor devices due to high temperature swing [1]. In medium and high-power applications, numerous wire-bonds are used in parallel to carry large currents. The lift-off of some, and not all wire-bonds significantly accelerate module ageing. Effectively, the current distribution constraint is dispatched onto the remaining connections. The early detection of this state of damage, defined as soft-failure or partial failure, is a challenge in pre-empting the catastrophic failure of the module. The failed device is where all bond-wires of an active device become disconnected. In this study, to produce the soft-faulty mode, power bond-wires connected to the emitter are manually and successively disconnected.

3. Healthy and Faulty modes characterization of the IGBT based assembly

3.1. Wide band analysis overview

The Z-parameters are obtained in both healthy and faulty modes through the measurements conducted in three configurations detailed in Table 1. In each configuration, the Z-parameters obtained are denoted as follows: Z_{11} for input impedance at port 1, Z_{12} for coupling impedance from port 1 to 2, Z_{21} for coupling impedance from port 2 to 1 and Z_{22} for input impedance at port 2.

Table 1 The 3 measurement configurations

	Port 1	Port 2	Grounded Port
Configuration 1	Collector	Emitter	Gate
Configuration 2	Gate	Collector	Emitter
Configuration 3	Emitter	Gate	Collector

The Fig. 2illustrates the measurement of Z_{11} in configuration 1 for healthy and faulty modes. The curves of faulty-modes are labelled based on the remaining bond-wires connected to the IGBT's emitter. It is notable that the general observations presented in this section are valid for all other Z-parameters.

The analysis of Fig. 2can be segmented into three distinct frequency bands based on the first and second resonant frequency f_1 and f_2, at $12\,MHz$ and $200\,MHz$.

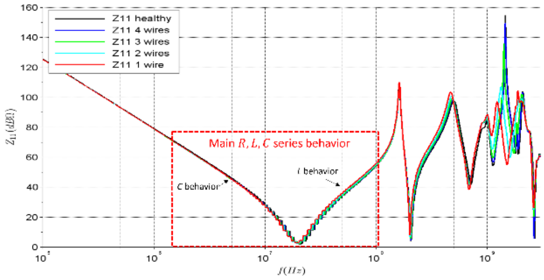

Fig. 2 Z11 in healthy mode and faulty modes

The capacitive behavior due to the off state of the IGBT is identifiable under f_1. Between f_1 and f_2, the inductive behavior is associated with the loop inductances of the module. At higher frequencies, a complex impedance behavior emerges due to the interplay between partial inductances and capacitors within the packaging. Notably, defects in bonding wires, which alter the associated partial inductance, are significantly observed at these higher frequencies. The first two frequency bands are briefly analyzed according to methodology detailed in [7] in the next section, while high frequencies are the focal point and the novelty of this study.

3.2. Low frequency analysis

Impedance analysis within the first two frequency bands provides significant information into both the IGBT and its packaging. By employing Z-parameters measured across the three configurations outlined in Table 1, equivalent R, L, C elements of the device can be derived. Consequently, a model can be constructed. C elements correspond mainly to the capacitances of the IGBT between the gate, collector, and emitter ports. R elements denote the serial resistances at these ports, influenced by both the internal characteristics of the IGBT and the packaging. L elements, representing serial inductances, are mainly influenced by the packaging. I in Table 2, the capacitance part obtained using this methodology is compared to two reference sources with a good agreement: C(V) measurements conducted with a curve tracer, specifically the B1505A Power Device Analyzer, and the capacitance values provided in the IGBT datasheet.

Table 2 Parasitic capacitance values (pF)

Parasitic Cap.	VNA charac. 1 MHz	Data sheet 1 MHz	B1505A 100 kHz
C_{GC}	1187	1010	1307
C_{GE}	2677	2390	2926
C_{CE}	545	690	398

Let us notice that all elements of the module contribute to the impedance below f_2. However, only overall R, L, and C elements can be computed, limiting these parameters as indicators of localized soft-failure. Notably, the lift-off of a single bond-wire results in only a minor variation of the global R and L elements, underscoring the importance of high-frequency analyses.

3.3. High frequency analysis

The impact of degradation is clearly discernible within the higher frequency range, in the third band above f_2 and partially between f_1 and f_2, as depicted in Fig. 2. However, the sensitivity of detection relies on the measurement configuration, the Z-parameter plotted, and the specific frequency considered within this frequency band. Henceforth, the objective is to consolidate these measurements into an effective indicator for efficiently detecting and localizing the degradation.

4. High frequency failure indicator

4.1. New Non-Destructive Testing characterization

Based on the two-ports Z-parameter characterizations, a failure indicator is constructed in 2 steps. The first step is to calculate the differential impedance Z_{diff} defined in eq.1. Z_{diff} represents the ratio between the differentially applied voltage across the tested ports and the resulting current flowing between them. This metric is particularly adapted to identify bond-wire lift-off occurrences within the current path linking the two ports. The comparison of Z_{diff} obtained in the 3 measurement configurations provides insights into fault localization. The second step employs the baselining method [8], subtracting the Z_{diff} measurement of a potentially faulty module from the $Z_{diff\_healthy}$ measurement in a healthy state, thus defining the fault indicator FI, as reported in eq.2.

$$Z_{diff} = Z_{11} + Z_{22} - Z_{21} - Z_{21} \quad (1)$$

$$FI = Z_{diff} - Z_{diff\_healthy} \quad (2)$$

As presented in [8], baselining enables a notable enhancement in the accuracy of detecting soft failures characterized by slight variations of electrical parameters. Furthermore, it can be demonstrated that FI is quasi-proportional to the fault impedance. This statement will be justified in the final paper.

4.2. Application of the failure indicator

FI given in Fig. 3 is computed onto the Z-parameters measurement in configuration 1, i.e from collector to emitter port. The successive lift-off failures are obviously detected in the higher frequency range $[200\ MHz - 2\ GHz]$ as explained previously. Where $f_1 < f < f_2$, the partial failure can be distinguished with a lower accuracy. Moreover, the magnitude of FI decreases in line with the degradation, showing no dependency on frequency and emphasizing the proportional property of FI.

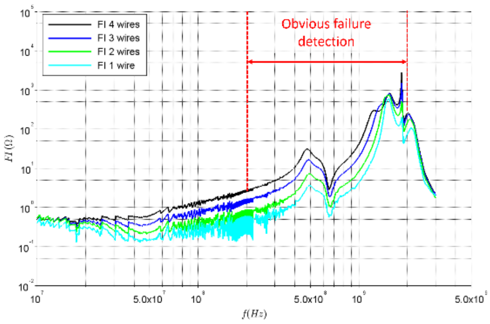

Fig. 3 FI computation in configuration 1

FI is also computed for the 3 measurement configurations as depicted in Fig. 4, considering only one bond-wire lift-off. This figure emphasizes that *FI* is notably higher for configurations 1 and 3 in the frequency range $f_1 < f < f_2$. The use of the 3 configurations of the NDT methodology enables to distinguish the impact of the failure regarding the different tested ports, giving discernible evidence on the failure localization.

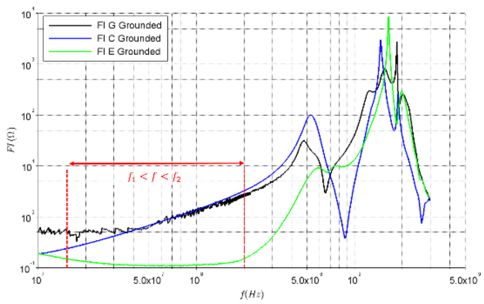

Fig. 4 Comparison of FI among the 3 measurement configurations

Finally, another device based on the same substrate without the IGBT and featuring an increased number of bond wires is tested. Specifically, 14 bond wires are connected from Track TG to Track TE. Bond-wire lift-off on this connection is so associated with an even lesser change in link impedance. A detailed analysis of the soft-failure detection on this device will be provided in the final paper. As a matter of facts, FI's effectiveness, will be highlighted.

5. Conclusions

A failure detection methodology has been developed based on impedance characterization across a wide frequency band and applied on an IGBT-based power module. By considering the analysis on both low and high frequency, potential failure modes could be distinguished. More precisely the lift-off detection of wire-bonds was illustrated. Thanks to a new high frequency indicator, it has been demonstrated the efficiency of the methodology even in a soft-faulty state. Future work will involve the identification of different failure mechanisms linked with IGBT solder or ceramic substrate.

Acknowledgements

Study funded by PIA-ANR-16-IDEX-0002, Energy and Solution for Environment project - E2S UPPA (France) within the framework of the EFICIENCE Chair (2020-2026).

References

[1] Ciappa M., Selected failure mechanisms of modern power modules, Microelectronics Reliability 42 (2002) PII: S00 2 6-2 7 14 (0 2)0 00 4 2- 2.

[2] Smet V. et al., Ageing and Failure Modes of IGBT Modules in High-Temperature Power Cycling, IEEE Transactions on Industrial Electronics, Vol. 58, N°. 10, October 2011, 4931-4941.

[3] Baffreau S., et.al., Wire bonding failure signature using high frequency characterization, EPE'19 ECCE Europe ISBN: 978-9-0758-1530-6, Genova Italy 2019.

[4] Jung D.H., et. al., Through silicon via (tsv) defect modeling, measurement, and analysis, IEEE Transactions on components, packaging and manufacturing technology, vol. 7, n°1, doi: 10.1109/TCPMT.2016.2631731, January 2017.

[5] Test & Measurement Application Note 95-1 S-Parameter Techniques, online 19/12/2022: www.ieee.li/pdf/viewgraphs/s_parameter_techniques.pdf

[6] Reveyrand T., Multiport conversions between S, Z, Y, h, ABCD, and T parameters 2018 International Workshop on Integrated Nonlinear Microwave and Millimeter-wave Circuits (INMMIC), Brive La Gaillarde, France, 2018, pp. 1-3, doi: 10.1109/INMMIC.2018.8430023.

[7] T. Liu, et. al., A New Characterization Technique for Extracting Parasitic Inductances of SiC Power Mosfets in Discrete and Module Packages Based on Two-Port S-Parameters Measurement, IEEE Transactions on Power Electronics, Vol. 33, N°11, November 2018.

[8] Kafal M. et al., Baselining: A Critical Approach Used for Soft Fault Detection in Wire Networks. International Journal of Digital Information and Wireless Communications (IJDIWC). 8. 52-57. 10.17781/P002405, (2018).